PHYSICAL REVIEW D **69**, 011103(R) (2004)

J/ψ production via initial state radiation in $e^+e^- \to \mu^+\mu^-\gamma$ at an e^+e^- center-of-mass energy near 10.6 GeV

B. Aubert,[1] R. Barate,[1] D. Boutigny,[1] J.-M. Gaillard,[1] A. Hicheur,[1] Y. Karyotakis,[1] J. P. Lees,[1] P. Robbe,[1] V. Tisserand,[1] A. Zghiche,[1] A. Palano,[2] A. Pompili,[2] J. C. Chen,[3] N. D. Qi,[3] G. Rong,[3] P. Wang,[3] Y. S. Zhu,[3] G. Eigen,[4] I. Ofte,[4] B. Stugu,[4] G. S. Abrams,[5] A. W. Borgland,[5] A. B. Breon,[5] D. N. Brown,[5] J. Button-Shafer,[5] R. N. Cahn,[5] E. Charles,[5] C. T. Day,[5] M. S. Gill,[5] A. V. Gritsan,[5] Y. Groysman,[5] R. G. Jacobsen,[5] R. W. Kadel,[5] J. Kadyk,[5] L. T. Kerth,[5] Yu. G. Kolomensky,[5] J. F. Kral,[5] G. Kukartsev,[5] C. LeClerc,[5] M. E. Levi,[5] G. Lynch,[5] L. M. Mir,[5] P. J. Oddone,[5] T. J. Orimoto,[5] M. Pripstein,[5] N. A. Roe,[5] A. Romosan,[5] M. T. Ronan,[5] V. G. Shelkov,[5] A. V. Telnov,[5] W. A. Wenzel,[5] K. Ford,[6] T. J. Harrison,[6] C. M. Hawkes,[6] D. J. Knowles,[6] S. E. Morgan,[6] R. C. Penny,[6] A. T. Watson,[6] N. K. Watson,[6] K. Goetzen,[7] T. Held,[7] H. Koch,[7] B. Lewandowski,[7] M. Pelizaeus,[7] K. Peters,[7] H. Schmuecker,[7] M. Steinke,[7] N. R. Barlow,[8] J. T. Boyd,[8] N. Chevalier,[8] W. N. Cottingham,[8] M. P. Kelly,[8] T. E. Latham,[8] C. Mackay,[8] F. F. Wilson,[8] K. Abe,[9] T. Cuhadar-Donszelmann,[9] C. Hearty,[9] T. S. Mattison,[9] J. A. McKenna,[9] D. Thiessen,[9] P. Kyberd,[10] A. K. McKemey,[10] V. E. Blinov,[11] A. D. Bukin,[11] V. P. Druzhinin,[11] V. B. Golubev,[11] V. N. Ivanchenko,[11] E. A. Kravchenko,[11] A. P. Onuchin,[11] S. I. Serednyakov,[11] Yu. I. Skovpen,[11] E. P. Solodov,[11] A. N. Yushkov,[11] D. Best,[12] M. Bruinsma,[12] M. Chao,[12] D. Kirkby,[12] A. J. Lankford,[12] M. Mandelkern,[12] R. K. Mommsen,[12] W. Roethel,[12] D. P. Stoker,[12] C. Buchanan,[13] B. L. Hartfiel,[13] B. C. Shen,[14] D. del Re,[15] H. K. Hadavand,[15] E. J. Hill,[15] D. B. MacFarlane,[15] H. P. Paar,[15] Sh. Rahatlou,[15] V. Sharma,[15] J. W. Berryhill,[16] C. Campagnari,[16] B. Dahmes,[16] N. Kuznetsova,[16] S. L. Levy,[16] O. Long,[16] A. Lu,[16] M. A. Mazur,[16] J. D. Richman,[16] W. Verkerke,[16] T. W. Beck,[17] J. Beringer,[17] A. M. Eisner,[17] C. A. Heusch,[17] W. S. Lockman,[17] T. Schalk,[17] R. E. Schmitz,[17] B. A. Schumm,[17] A. Seiden,[17] M. Turri,[17] W. Walkowiak,[17] D. C. Williams,[17] M. G. Wilson,[17] J. Albert,[18] E. Chen,[18] G. P. Dubois-Felsmann,[18] A. Dvoretskii,[18] D. G. Hitlin,[18] I. Narsky,[18] F. C. Porter,[18] A. Ryd,[18] A. Samuel,[18] S. Yang,[18] S. Jayatilleke,[19] G. Mancinelli,[19] B. T. Meadows,[19] M. D. Sokoloff,[19] T. Abe,[20] F. Blanc,[20] P. Bloom,[20] S. Chen,[20] P. J. Clark,[20] W. T. Ford,[20] U. Nauenberg,[20] A. Olivas,[20] P. Rankin,[20] J. Roy,[20] J. G. Smith,[20] W. C. van Hoek,[20] L. Zhang,[20] J. L. Harton,[21] T. Hu,[21] A. Soffer,[21] W. H. Toki,[21] R. J. Wilson,[21] J. Zhang,[21] D. Altenburg,[22] T. Brandt,[22] J. Brose,[22] T. Colberg,[22] M. Dickopp,[22] R. S. Dubitzky,[22] A. Hauke,[22] H. M. Lacker,[22] E. Maly,[22] R. Müller-Pfefferkorn,[22] R. Nogowski,[22] S. Otto,[22] J. Schubert,[22] K. R. Schubert,[22] R. Schwierz,[22] B. Spaan,[22] L. Wilden,[22] D. Bernard,[23] G. R. Bonneaud,[23] F. Brochard,[23] J. Cohen-Tanugi,[23] P. Grenier,[23] Ch. Thiebaux,[23] G. Vasileiadis,[23] M. Verderi,[23] A. Khan,[24] D. Lavin,[24] F. Muheim,[24] S. Playfer,[24] J. E. Swain,[24] M. Andreotti,[25] V. Azzolini,[25] D. Bettoni,[25] C. Bozzi,[25] R. Calabrese,[25] G. Cibinetto,[25] E. Luppi,[25] M. Negrini,[25] L. Piemontese,[25] A. Sarti,[25] E. Treadwell,[26] F. Anulli,[27,*] R. Baldini-Ferroli,[27] M. Biasini,[27,*] A. Calcaterra,[27] R. de Sangro,[27] D. Falciai,[27] G. Finocchiaro,[27] P. Patteri,[27] I. M. Peruzzi,[27,*] M. Piccolo,[27] M. Pioppi,[27,*] A. Zallo,[27] A. Buzzo,[28] R. Capra,[28] R. Contri,[28] G. Crosetti,[28] M. Lo Vetere,[28] M. Macri,[28] M. R. Monge,[28] S. Passaggio,[28] C. Patrignani,[28] E. Robutti,[28] A. Santroni,[28] S. Tosi,[28] S. Bailey,[28] M. Morii,[29] E. Won,[29] W. Bhimji,[30] D. A. Bowerman,[30] P. D. Dauncey,[30] U. Egede,[30] I. Eschrich,[30] J. R. Gaillard,[30] G. W. Morton,[30] J. A. Nash,[30] P. Sanders,[30] G. P. Taylor,[30] G. J. Grenier,[31] S.-J. Lee,[31] U. Mallik,[31] J. Cochran,[32] H. B. Crawley,[32] J. Lamsa,[32] W. T. Meyer,[32] S. Prell,[32] E. I. Rosenberg,[32] J. Yi,[32] M. Davier,[33] G. Grosdidier,[33] A. Höcker,[33] S. Laplace,[33] F. Le Diberder,[33] V. Lepeltier,[33] A. M. Lutz,[33] T. C. Petersen,[33] S. Plaszczynski,[33] M. H. Schune,[33] L. Tantot,[33] G. Wormser,[33] V. Brigljević,[34] C. H. Cheng,[34] D. J. Lange,[34] D. M. Wright,[34] A. J. Bevan,[35] J. P. Coleman,[35] J. R. Fry,[35] E. Gabathuler,[35] R. Gamet,[35] M. Kay,[35] R. J. Parry,[35] D. J. Payne,[35] R. J. Sloane,[35] C. Touramanis,[35] J. J. Back,[36] P. F. Harrison,[36] H. W. Shorthouse,[36] P. Strother,[36] P. B. Vidal,[36] C. L. Brown,[37] G. Cowan,[37] R. L. Flack,[37] H. U. Flaecher,[37] S. George,[37] M. G. Green,[37] A. Kurup,[37] C. E. Marker,[37] T. R. McMahon,[37] S. Ricciardi,[37] F. Salvatore,[37] G. Vaitsas,[37] M. A. Winter,[37] D. Brown,[38] C. L. Davis,[38] J. Allison,[39] R. J. Barlow,[39] A. C. Forti,[39] P. A. Hart,[39] M. C. Hodgkinson,[39] F. Jackson,[39] G. D. Lafferty,[39] A. J. Lyon,[39] J. H. Weatherall,[39] J. C. Williams,[39] A. Farbin,[40] A. Jawahery,[40] D. Kovalskyi,[40] C. K. Lae,[40] V. Lillard,[40] D. A. Roberts,[40] G. Blaylock,[41] C. Dallapiccola,[41] K. T. Flood,[41] S. S. Hertzbach,[41] R. Kofler,[41] V. B. Koptchev,[41] T. B. Moore,[41] S. Saremi,[41] H. Staengle,[41] S. Willocq,[41] R. Cowan,[42] G. Sciolla,[42] F. Taylor,[42] R. K. Yamamoto,[42] D. J. J. Mangeol,[43] P. M. Patel,[43] A. Lazzaro,[44] F. Palombo,[44] J. M. Bauer,[45] L. Cremaldi,[45] V. Eschenburg,[45] R. Godang,[45] R. Kroeger,[45] J. Reidy,[45] D. A. Sanders,[45] D. J. Summers,[45] H. W. Zhao,[45] S. Brunet,[46] D. Cote-Ahern,[46] C. Hast,[46] P. Taras,[46] H. Nicholson,[47] C. Cartaro,[48] N. Cavallo,[48,†] G. De Nardo,[48] F. Fabozzi,[48,†] C. Gatto,[48] L. Lista,[48] P. Paolucci,[48] D. Piccolo,[48] C. Sciacca,[48] M. A. Baak,[49] G. Raven,[49] J. M. LoSecco,[50] T. A. Gabriel,[51] B. Brau,[52] K. K. Gan,[52] K. Honscheid,[52] D. Hufnagel,[52] H. Kagan,[52] R. Kass,[52] T. Pulliam,[52] Q. K. Wong,[52] J. Brau,[53] R. Frey,[53] C. T. Potter,[53] N. B. Sinev,[53] D. Strom,[53] E. Torrence,[53] F. Colecchia,[54] A. Dorigo,[54] F. Galeazzi,[54] M. Margoni,[54] M. Morandin,[54] M. Posocco,[54] M. Rotondo,[54] F. Simonetto,[54] R. Stroili,[54] G. Tiozzo,[54] C. Voci,[54] M. Benayoun,[55] H. Briand,[55] J. Chauveau,[55] P. David,[55] Ch. de la Vaissière,[55] L. Del Buono,[55] O. Hamon,[55] M. J. J. John,[55] Ph. Leruste,[55] J. Ocariz,[55] M. Pivk,[55] L. Roos,[55] J. Stark,[55] S. T'Jampens,[55] G. Therin,[55] P. F. Manfredi,[56] V. Re,[56] P. K. Behera,[57] L. Gladney,[57] Q. H. Guo,[57] J. Panetta,[57] C. Angelini,[58] G. Batignani,[58] S. Bettarini,[58] M. Bondioli,[58] F. Bucci,[58] G. Calderini,[58] M. Carpinelli,[58] V. Del Gamba,[58] F. Forti,[58] M. A. Giorgi,[58] A. Lusiani,[58] G. Marchiori,[58] F. Martinez-Vidal,[58,‡] M. Morganti,[58] N. Neri,[58] E. Paoloni,[58] M. Rama,[58] G. Rizzo,[58] F. Sandrelli,[58] J. Walsh,[58] M. Haire,[59] D. Judd,[59] K. Paick,[59] D. E. Wagoner,[59] N. Danielson,[60] P. Elmer,[60] C. Lu,[60] V. Miftakov,[60] J. Olsen,[60] A. J. S. Smith,[60] H. A. Tanaka,[60] E. W. Varnes,[60] F. Bellini,[61] G. Cavoto,[60,61] R. Faccini,[15,61]

F. Ferrarotto,[61] F. Ferroni,[61] M. Gaspero,[61] M. A. Mazzoni,[61] S. Morganti,[61] M. Pierini,[61] G. Piredda,[61] F. Safai Tehrani,[61] C. Voena,[61] S. Christ,[62] G. Wagner,[62] R. Waldi,[62] T. Adye,[63] N. De Groot,[63] B. Franek,[63] N. I. Geddes,[63] G. P. Gopal,[63] E. O. Olaiya,[63] S. M. Xella,[63] R. Aleksan,[64] S. Emery,[64] A. Gaidot,[64] S. F. Ganzhur,[64] P.-F. Giraud,[64] G. Hamel de Monchenault,[64] W. Kozanecki,[64] M. Langer,[64] M. Legendre,[64] G. W. London,[64] B. Mayer,[64] G. Schott,[64] G. Vasseur,[64] Ch. Yeche,[64] M. Zito,[64] M. V. Purohit,[65] A. W. Weidemann,[65] F. X. Yumiceva,[65] D. Aston,[66] R. Bartoldus,[66] N. Berger,[66] A. M. Boyarski,[66] O. L. Buchmueller,[66] M. R. Convery,[66] D. P. Coupal,[66] D. Dong,[66] J. Dorfan,[66] D. Dujmic,[66] W. Dunwoodie,[66] R. C. Field,[66] T. Glanzman,[66] S. J. Gowdy,[66] E. Grauges-Pous,[66] T. Hadig,[66] V. Halyo,[66] T. Hryn'ova,[66] W. R. Innes,[66] C. P. Jessop,[66] M. H. Kelsey,[66] P. Kim,[66] M. L. Kocian,[66] U. Langenegger,[66] D. W. G. S. Leith,[66] S. Luitz,[66] V. Luth,[66] H. L. Lynch,[66] H. Marsiske,[66] R. Messner,[66] D. R. Muller,[66] C. P. O'Grady,[66] V. E. Ozcan,[66] A. Perazzo,[66] M. Perl,[66] S. Petrak,[66] B. N. Ratcliff,[66] S. H. Robertson,[66] A. Roodman,[66] A. A. Salnikov,[66] R. H. Schindler,[66] J. Schwiening,[66] G. Simi,[66] A. Snyder,[66] A. Soha,[66] J. Stelzer,[66] D. Su,[66] M. K. Sullivan,[66] J. Va'vra,[66] S. R. Wagner,[66] M. Weaver,[66] A. J. R. Weinstein,[66] W. J. Wisniewski,[66] D. H. Wright,[66] C. C. Young,[66] P. R. Burchat,[67] A. J. Edwards,[67] T. I. Meyer,[67] B. A. Petersen,[67] C. Roat,[67] S. Ahmed,[68] M. S. Alam,[68] J. A. Ernst,[68] M. Saleem,[68] F. R. Wappler,[68] W. Bugg,[69] M. Krishnamurthy,[69] S. M. Spanier,[69] R. Eckmann,[70] H. Kim,[70] J. L. Ritchie,[70] R. F. Schwitters,[70] J. M. Izen,[71] I. Kitayama,[71] X. C. Lou,[71] S. Ye,[71] F. Bianchi,[72] M. Bona,[72] F. Gallo,[72] D. Gamba,[72] C. Borean,[73] L. Bosisio,[73] G. Della Ricca,[73] S. Dittongo,[73] S. Grancagnolo,[73] L. Lanceri,[73] P. Poropat,[73,§] L. Vitale,[73] G. Vuagnin,[73] R. S. Panvini,[74] Sw. Banerjee,[75] C. M. Brown,[75] D. Fortin,[75] P. D. Jackson,[75] R. Kowalewski,[75] J. M. Roney,[75] H. R. Band,[76] S. Dasu,[76] M. Datta,[76] A. M. Eichenbaum,[76] J. R. Johnson,[76] P. E. Kutter,[76] H. Li,[76] R. Liu,[76] F. Di Lodovico,[76] A. Mihalyi,[76] A. K. Mohapatra,[76] Y. Pan,[76] R. Prepost,[76] S. J. Sekula,[76] J. H. von Wimmersperg-Toeller,[76] J. Wu,[76] S. L. Wu,[76] Z. Yu,[76] and H. Neal[77]

(BABAR Collaboration)

[1]*Laboratoire de Physique des Particules, F-74941 Annecy-le-Vieux, France*
[2]*Università di Bari, Dipartimento di Fisica and INFN, I-70126 Bari, Italy*
[3]*Institute of High Energy Physics, Beijing 100039, China*
[4]*University of Bergen, Inst. of Physics, N-5007 Bergen, Norway*
[5]*Lawrence Berkeley National Laboratory and University of California, Berkeley, California 94720, USA*
[6]*University of Birmingham, Birmingham, B15 2TT, United Kingdom*
[7]*Ruhr Universität Bochum, Institut für Experimentalphysik 1, D-44780 Bochum, Germany*
[8]*University of Bristol, Bristol BS8 1TL, United Kingdom*
[9]*University of British Columbia, Vancouver, British Columbia, Canada V6T 1Z1*
[10]*Brunel University, Uxbridge, Middlesex UB8 3PH, United Kingdom*
[11]*Budker Institute of Nuclear Physics, Novosibirsk 630090, Russia*
[12]*University of California at Irvine, Irvine, California 92697, USA*
[13]*University of California at Los Angeles, Los Angeles, California 90024, USA*
[14]*University of California at Riverside, Riverside, California 92521, USA*
[15]*University of California at San Diego, La Jolla, California 92093, USA*
[16]*University of California at Santa Barbara, Santa Barbara, California 93106, USA*
[17]*University of California at Santa Cruz, Institute for Particle Physics, Santa Cruz, California 95064, USA*
[18]*California Institute of Technology, Pasadena, California 91125, USA*
[19]*University of Cincinnati, Cincinnati, Ohio 45221, USA*
[20]*University of Colorado, Boulder, Colorado 80309, USA*
[21]*Colorado State University, Fort Collins, Colorado 80523, USA*
[22]*Technische Universität Dresden, Institut für Kern- und Teilchenphysik, D-01062 Dresden, Germany*
[23]*Ecole Polytechnique, LLR, F-91128 Palaiseau, France*
[24]*University of Edinburgh, Edinburgh EH9 3JZ, United Kingdom*
[25]*Università di Ferrara, Dipartimento di Fisica and INFN, I-44100 Ferrara, Italy*
[26]*Florida A&M University, Tallahassee, Florida 32307, USA*
[27]*Laboratori Nazionali di Frascati dell'INFN, I-00044 Frascati, Italy*
[28]*Università di Genova, Dipartimento di Fisica and INFN, I-16146 Genova, Italy*
[29]*Harvard University, Cambridge, Massachusetts 02138, USA*
[30]*Imperial College London, London, SW7 2BW, United Kingdom*
[31]*University of Iowa, Iowa City, Iowa 52242, USA*
[32]*Iowa State University, Ames, Iowa 50011-3160, USA*
[33]*Laboratoire de l'Accélérateur Linéaire, F-91898 Orsay, France*
[34]*Lawrence Livermore National Laboratory, Livermore, California 94550, USA*
[35]*University of Liverpool, Liverpool L69 3BX, United Kingdom*
[36]*Queen Mary, University of London, E1 4NS, United Kingdom*
[37]*University of London, Royal Holloway and Bedford New College, Egham, Surrey TW20 0EX, United Kingdom*

[38]*University of Louisville, Louisville, Kentucky 40292, USA*
[39]*University of Manchester, Manchester M13 9PL, United Kingdom*
[40]*University of Maryland, College Park, Maryland 20742, USA*
[41]*University of Massachusetts, Amherst, Massachusetts 01003, USA*
[42]*Massachusetts Institute of Technology, Laboratory for Nuclear Science, Cambridge, Massachusettes 02139, USA*
[43]*McGill University, Montréal, Quebec, Canada H3A 2T8*
[44]*Università di Milano, Dipartimento di Fisica and INFN, I-20133 Milano, Italy*
[45]*University of Mississippi, University, Mississippi 38677, USA*
[46]*Université de Montréal, Laboratoire René J. A. Lévesque, Montréal, Quebec, Canada H3C 3J7*
[47]*Mount Holyoke College, South Hadley, Massachusetts 01075, USA*
[48]*Università di Napoli Federico II, Dipartimento di Scienze Fisiche and INFN, I-80126, Napoli, Italy*
[49]*NIKHEF, National Institute for Nuclear Physics and High Energy Physics, NL-1009 DB Amsterdam, The Netherlands*
[50]*University of Notre Dame, Notre Dame, Indiana 46556, USA*
[51]*Oak Ridge National Laboratory, Oak Ridge, Tennessee 37831, USA*
[52]*Ohio State University, Columbus, Ohio 43210, USA*
[53]*University of Oregon, Eugene, Oregon 97403, USA*
[54]*Università di Padova, Dipartimento di Fisica and INFN, I-35131 Padova, Italy*
[55]*Universités Paris VI et VII, Lab de Physique Nucléaire H. E., F-75252 Paris, France*
[56]*Università di Pavia, Dipartimento di Elettronica and INFN, I-27100 Pavia, Italy*
[57]*University of Pennsylvania, Philadelphia, Pennsylvania 19104, USA*
[58]*Università di Pisa, Dipartimento di Fisica, Scuola Normale Superiore and INFN, I-56127 Pisa, Italy*
[59]*Prairie View A&M University, Prairie View, Texas 77446, USA*
[60]*Princeton University, Princeton, New Jersey 08544, USA*
[61]*Università di Roma La Sapienza, Dipartimento di Fisica and INFN, I-00185 Roma, Italy*
[62]*Universität Rostock, D-18051 Rostock, Germany*
[63]*Rutherford Appleton Laboratory, Chilton, Didcot, Oxon, OX11 0QX, United Kingdom*
[64]*DSM/Dapnia, CEA/Saclay, F-91191 Gif-sur-Yvette, France*
[65]*University of South Carolina, Columbia, South Carolina 29208, USA*
[66]*Stanford Linear Accelerator Center, Stanford, California 94309, USA*
[67]*Stanford University, Stanford, California 94305-4060, USA*
[68]*State Univ. of New York, Albany, New York 12222, USA*
[69]*University of Tennessee, Knoxville, Tennessee 37996, USA*
[70]*University of Texas at Austin, Austin, Texas 78712, USA*
[71]*University of Texas at Dallas, Richardson, Texas 75083, USA*
[72]*Università di Torino, Dipartimento di Fisica Sperimentale and INFN, I-10125 Torino, Italy*
[73]*Università di Trieste, Dipartimento di Fisica and INFN, I-34127 Trieste, Italy*
[74]*Vanderbilt University, Nashville, Tennessee 37235, USA*
[75]*University of Victoria, Victoria, British Columbia, Canada V8W 3P6*
[76]*University of Wisconsin, Madison, Wisconsin 53706, USA*
[77]*Yale University, New Haven, Connecticut 06511, USA*

(Received 14 October 2003; published 30 January 2004)

We have studied the process $e^+e^-\to\mu^+\mu^-\gamma$ at a center-of-mass energy near the $\Upsilon(4S)$ resonance for a $\mu^+\mu^-$ invariant mass range near the J/ψ mass and measured the cross section $\sigma(e^+e^-\to J/\psi\,\gamma\to\mu^+\mu^-\gamma)$. The data set, corresponding to an integrated luminosity of 88.4 fb^{-1}, was collected using the BABAR detector at the SLAC PEP-II collider. From the measured cross section we extract the product $\Gamma(J/\psi\to e^+e^-)B(J/\psi\to\mu^+\mu^-)=0.330\pm0.008\pm0.007$ keV. Using the world averages for $B(J/\psi\to\mu^+\mu^-)$ and $B(J/\psi\to e^+e^-)$, we derive the J/ψ electronic and total widths: $\Gamma(J/\psi\to e^+e^-)=5.61\pm0.20$ keV and $\Gamma=94.7\pm4.4$ keV.

DOI: 10.1103/PhysRevD.69.011103 PACS number(s): 13.20.Gd, 13.66.Bc, 14.40.Gx

The possibility of using e^+e^- annihilation with initial state radiation (ISR), $e^+e^-\to$hadrons$+\gamma$, to measure the e^+e^- cross sections into hadrons over a wide range of center-of-mass (c.m.) energies in a single experiment has been discussed in the literature [1]. In this paper, we have implemented this idea by studying the process $e^+e^-\to\mu^+\mu^-\gamma$ for $\mu^+\mu^-$ masses in the range from 2.8 to 3.4 GeV/c^2. We measure the cross section $\sigma(e^+e^-\to J/\psi\,\gamma\to\mu^+\mu^-\gamma)$ and derive the product of electronic

*Also with Università di Perugia, Perugia, Italy.
†Also with Università della Basilicata, Potenza, Italy.
‡Also with IFIC, Instituto de Física Corpuscular, CSIC-Universidad de Valencia, Valencia, Spain.
§Deceased.

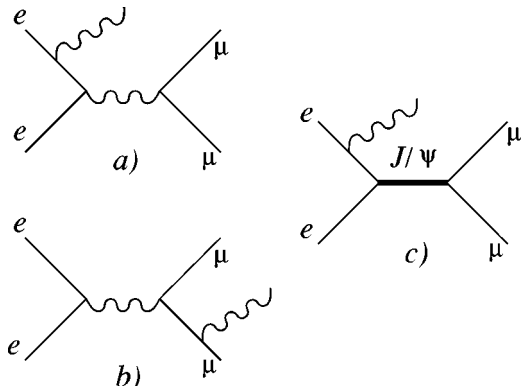

FIG. 1. Diagrams for $e^+e^-\to\mu^+\mu^-\gamma$. (a) Initial state radiation. (b) Final state radiation. (c) J/ψ production.

width times the branching fraction $\Gamma(J/\psi\to e^+e^-)B(J/\psi\to\mu^+\mu^-)$. Using the world averages for $B(J/\psi\to\mu^+\mu^-)$ and $B(J/\psi\to e^+e^-)$ [2], we then derive the electronic and total widths of the J/ψ meson. The data used in this analysis were collected with the BABAR detector [3] at the SLAC PEP-II asymmetric e^+e^- storage ring [4].

The Born cross section for the process $e^+e^-\to\mu^+\mu^-\gamma$ in the J/ψ mass region has contributions from three Feynman diagrams, as illustrated in Fig. 1. The first and second of these diagrams describe the pure QED processes corresponding to initial state radiation and final state radiation (FSR). The visible QED cross section in *BABAR* (defined by our ISR photon acceptance) is about 1.2 pb in the di-muon mass range 2.8–3.4 GeV/c^2. The contribution of the FSR process to the QED cross section depends on the photon energy and angle, and is about 10–20 % for the kinematic regime we study. The interference between ISR and FSR amplitudes does not change the total cross section, but leads to charge asymmetries in the muon angular distributions.

The Born cross section for J/ψ production [Fig. 1c] is given by

$$\frac{d\sigma^{\rm Born}_{J/\psi}(s,x)}{dx}=W(s,x)\sigma_0(s(1-x)), \tag{1}$$

where $\sqrt{s}$ is the e^+e^- invariant mass, $x\equiv 2E_\gamma/\sqrt{s}$, E_γ is the photon energy in the c.m., and σ_0 is the Born cross section for $e^+e^-\to J/\psi\to\mu^+\mu^-$. The function

$$W(s,x)=\frac{2\alpha}{\pi x}\left(2\ln\frac{\sqrt{s}}{m_e}-1\right)\left(1-x+\frac{x^2}{2}\right) \tag{2}$$

describes the probability of ISR photon emission. Here α is the fine structure constant and m_e is the electron mass. ISR photons are emitted predominantly at small angles relative to the electron direction. About 10% of the photons have c.m. polar angles in the range $30°<\theta<150°$ and can be detected in *BABAR*.

As a first approximation, the Born cross section for $e^+e^-\to J/\psi\to\mu^+\mu^-$ is given by the Breit-Wigner formula

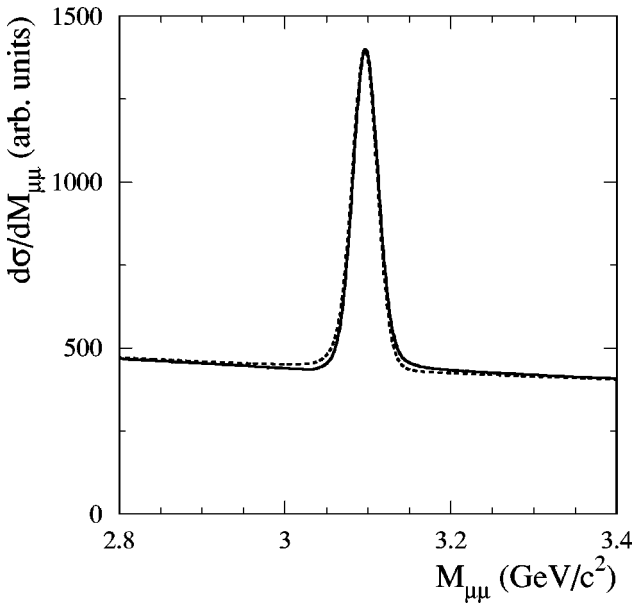

FIG. 2. The di-muon mass spectrum calculated with (solid line) and without (dashed line) interference between the resonant J/ψ production and QED amplitudes after convolution with the detector resolution function.

$$\sigma_0(s)=\frac{12\pi B_{ee}B_{\mu\mu}}{m^2}\frac{m^2\Gamma^2}{(s-m^2)^2+m^2\Gamma^2}, \tag{3}$$

where m and Γ are the J/ψ mass and total width, respectively, B_{ee} and $B_{\mu\mu}$ are the branching fractions $B(J/\psi\to e^+e^-)$ and $B(J/\psi\to\mu^+\mu^-)$. For a narrow resonance, such as the J/ψ, we can replace the Breit-Wigner with a δ function $\pi m\Gamma\,\delta(s-m^2)$ and integrate over photon energy to find

$$\sigma^{\rm Born}_{J/\psi}(s)=\frac{12\pi^2\Gamma_{ee}B_{\mu\mu}}{m\cdot s}W(s,x_0),\quad x_0=1-\frac{m^2}{s}. \tag{4}$$

Here $\Gamma_{ee}=\Gamma\cdot B_{ee}$. These formulas do not account for interference between the $e^+e^-\to J/\psi\to\mu^+\mu^-$ and the nonresonant (QED) $e^+e^-\to\mu^+\mu^-$ amplitudes.

The cross section for $e^+e^-\to\mu^+\mu^-$ including QED and resonant J/ψ production amplitudes and their interference can be written as [5]

$$\sigma(s)=\frac{4\pi\alpha^2}{3s}\left|1-Q\frac{m\Gamma}{m^2-s-im\Gamma}\right|^2, \tag{5}$$

where $Q=3\sqrt{B_{ee}B_{\mu\mu}}/\alpha$. The interference term changes sign at the J/ψ mass. Therefore, it does not change the integrated cross section of Eq. (4) significantly, but does change the shape of the mass distribution. Because the J/ψ cross section is so much greater than the QED cross section at resonance ($Q^2\approx 600$), the power-law behavior of the Breit-Wigner tails produces observable interference even 1000 widths from resonance. The expected di-muon mass spectrum, convolved with the detector resolution, is shown in Fig. 2. The interference is clearly seen, despite the experimental resolution,

14.5 MeV/c^2, being more than 100 times the J/ψ natural linewidth. The maximum relative difference between the spectra calculated with and without interference is about 7%. The interference also leads to a 1.3 MeV/c^2 shift between the maximum of the resonance peak and the actual J/ψ mass. The shape of the expected mass spectrum is very sensitive to the tails of the Breit-Wigner approximation used in Eqs. (3) and (5), where its validity far from resonance is questionable. To estimate the sensitivity of our analysis to the details of the shape assumptions, we will take the full difference between fits that do, and do not, use interference as a measure of the systematic uncertainty.

The width of the J/ψ has been measured directly in $p\bar{p}$ annihilation with the result $99\pm12\pm6$ keV [6]. In e^+e^- annihilation, measuring the area under the resonance curve for $e^+e^-\to J/\psi\to\mu^+\mu^-$ gives the product $\Gamma_{ee}B_{\mu\mu}$ as seen in Eq. (4). Combining this with the leptonic branching ratio yields the total width. The BES Collaboration made a comprehensive collection of measurements at the J/ψ from which they determined $\Gamma=84.4\pm8.9$ keV [7]. This superseded results obtained from original measurements made of the area under the excitation curve in 1975. More recently, the BES Collaboration has measured the leptonic branching ratio with a 1.5% uncertainty using J/ψ's from the decay $\psi(2S)\to J/\psi\pi\pi$ [8]. It is this result that we combine with our measurement of $\Gamma_{ee}B_{\mu\mu}$ to obtain the highest precision result to date for the total width of the J/ψ.

Charged particle tracking for the BABAR detector is provided by a five-layer silicon vertex tracker (SVT) and a 40-layer drift chamber (DCH), operating in a 1.5 T axial magnetic field. The transverse momentum resolution is 0.47% at 1 GeV/c. Energies of photons and electrons are measured by a CsI(Tl) electromagnetic calorimeter (EMC) with resolution of 3% at 1 GeV. Charged particle identification is provided by ionization measurements in the SVT and DCH, and by an internally reflecting ring-imaging Cherenkov detector (DIRC). Muons are identified in the solenoid's instrumented flux return (IFR), which consists of iron plates interleaved with resistive plate chambers. The data sample used for this analysis corresponds to an integrated luminosity of 88.4 fb^{-1} recorded in the vicinity of the $\Upsilon(4S)$ resonance.

The initial selection of $\mu^+\mu^-\gamma$ candidates requires that all particles are detected inside a fiducial volume and that the event kinematics are consistent with the hypothesis $e^+e^-\to\mu^+\mu^-\gamma$. Photons must have polar angles in the range $0.35<\theta<2.4$ radians and must have a c.m. energy above 3 GeV. Muon candidates must have polar angles in the range $0.35<\theta<2.4$ radians and transverse momenta above 0.1 GeV/c, and must originate from the interaction point. Energy and momentum balance is provided by the conditions $|E_{\rm total}-E_{\rm beams}|<1.5$ GeV and $\Delta\Psi<0.07$. Here $E_{\rm total}$ is the summed energy of the muon candidates and the photon, $\Delta\Psi$ is the angle between the photon and the direction of the di-muon missing momentum, $\mathbf{p}_{\rm miss}\equiv\mathbf{p}_{e^+}+\mathbf{p}_{e^-}-\mathbf{p}_{\mu^+}-\mathbf{p}_{\mu^-}$. We reduce backgrounds using a one-constraint fit to the hypothesis that the recoil mass against the di-muon is zero. Requiring $\chi^2<20$ rejects 90% of the multihadron ISR contamination (general $e^+e^-\to q\bar{q}\gamma$ reactions) and about 10% of signal events.

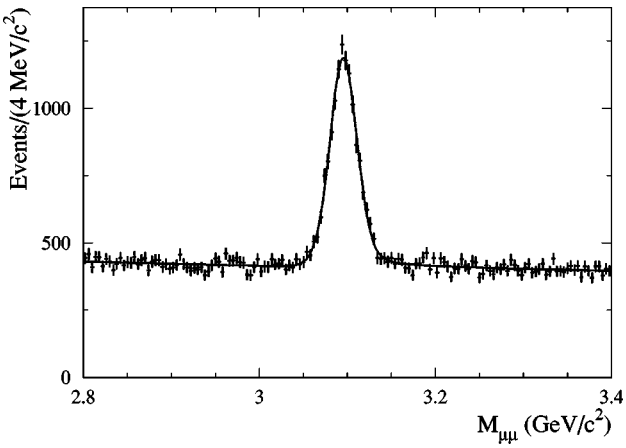

FIG. 3. The mass spectrum for observed events. The curve is the result of the fit described in the text.

The large background from $e^+e^-\to e^+e^-\gamma$ is suppressed by requiring that the charged track momenta be greater than 0.5 GeV/c and that the corresponding energies detected in the calorimeter be small: $E_{\rm EMC}<0.4$ GeV for each track. The average energy deposition of muons in the calorimeter is about 0.2 GeV, while electrons typically deposit more than 90% of their energy in the calorimeter. Additional suppression of this background is achieved by requiring large angular separation (in the c.m.) between the charged tracks and the photon ($\cos\theta^*_{\mu\gamma}<0.5$). This also reduces the level of FSR $\mu^+\mu^-\gamma$ events in the final sample by a factor of two. The invariant mass distribution of approximately 70000 di-muon pairs in our final sample is shown in Fig. 3. About 7800 events are in the J/ψ peak.

The remaining electron contamination in our final sample is estimated using a subsample of events enriched with electrons. To select this subsample we require that neither muon be identified in the IFR. Muon identification requires that a track penetrate at least 2 nuclear interaction lengths (λ) of IFR material, and that the difference between the measured and expected muon ranges be less than 2λ. This algorithm is 90% efficient for true muons and misidentifies about 10% of real electrons as muons. We then require that the DCH based dE/dx measurements for the two tracks be consistent with the di-electron hypothesis and inconsistent with the di-muon hypothesis. This eliminates 95% of di-muons and retains 85% of di-electrons. From the number of electron events in the selected subsample we estimate the fraction of electron events in the full sample to be $(0.1\pm0.1)\%$.

ISR events with hadronic final states are another source of background, both on resonance and off. For $e^+e^-\to J/\psi\,\gamma\to\pi^+\pi^-\gamma$ and $e^+e^-\to J/\psi\,\gamma\to K^+K^-\gamma$, the cross sections are proportional to the ratios of branching fractions $B(J/\psi\to\pi^+\pi^-)/B(J/\psi\to\mu^+\mu^-)\approx2.5\times10^{-3}$ and $B(J/\psi\to K^+K^-)/B(J/\psi\to\mu^+\mu^-)\approx4\times10^{-3}$. To first approximation, the off-resonance ratios, $\sigma(e^+e^-\to\pi^+\pi^-)/\sigma(e^+e^-\to\mu^+\mu^-)$ and $\sigma(e^+e^-\to K^+K^-)/\sigma(e^+e^-\to\mu^+\mu^-)$ are similar to those on resonance. As off-resonance production proceeds via virtual photon intermediate states while on-resonance production proceeds via both virtual photon intermediate states and hadronic intermediate states [9], the on-

resonance ratios are overestimates of the off-resonance ratios. Thus, we consider the on-resonance background rate as an upper limit for both.

The suppression of kaon and pion reactions was studied using samples of $e^+e^-\to\omega\gamma\to3\pi\gamma$ and $e^+e^-\to\phi\gamma\to K^+K^-\gamma$ events. About two thirds of these events are rejected by the calorimeter energy deposition requirement. Under the di-muon hypothesis, the peak of the $J/\psi\to K^+K^-$ distribution transforms into a broad distribution with $M_{\mu\mu}<2.95$ GeV/c^2. The only background peaking under the $J/\psi\to\mu^+\mu^-$ signal is that due to $J/\psi\to\pi^+\pi^-$; its contribution is estimated to be $(0.09\pm0.03)\%$. The only other decay into two charged hadrons, $J/\psi\to p\bar{p}$, produces events with $M_{\mu\mu}<2.4$ GeV/c^2, and thus contributes no background in the di-muon mass range studied here. The total nonresonant background from $e^+e^-\to e^+e^-\gamma$, $\pi^+\pi^-\gamma$, $K^+K^-\gamma$ processes is estimated to be $(0.3\pm0.2)\%$.

The background from ISR production of higher multiplicity multihadron events is estimated from Monte Carlo simulation. We estimate the background from multihadron J/ψ decays to be less than 0.05% using simulated $e^+e^-\to J/\psi\,\gamma$, $J/\psi\to3\pi$ events and J/ψ charged particle multiplicity data [8]. We also note that such events populate the mass region below 3 GeV/c^2 when misidentified as signal events. We use the JETSET [10] event generator to simulate the hadronic part of the $e^+e^-\to q\bar{q}\gamma$, $q=u,d,s$ cross section. We find the background due to such events to be less than 0.3%. As these background rates are not the dominant sources of systematic uncertainty in our final results, we have not tried to determine them with greater precision.

We use a binned maximum likelihood fit to describe the mass spectrum of Fig. 3. The mass range used, 2.8–3.4 GeV/c^2, is divided into 150 bins of width 4 MeV/c^2. The probability density function (PDF) for the J/ψ signal is modeled as the convolution of a J/ψ Breit-Wigner line shape and the resolution function shown in Fig. 4. This is derived from detector simulation in conjunction with an $e^+e^-\to\mu^+\mu^-\gamma$ event generator based on the differential cross sections of Ref. [11]. Soft photon radiation is generated with the use of the structure function method of Ref. [12] and the PHOTOS package [13] for electron and muon bremsstrahlung, respectively. Muon bremsstrahlung leads to the low mass tail observed in the spectrum of Fig. 4. To account for possible resolution differences between simulation and data, the resolution function shown in Fig. 4 is convolved with an additional Gaussian smearing function of width σ_G. Both σ_G and the observed J/ψ peak position, $M_{J/\psi}$, are parameters in our fit. A Monte Carlo calculation shows that the shape of the nonresonant cross section can be described well by a linear function. To account for possible deviations from this hypothesis (e.g., due to detector response) a second-order polynomial is used to fit the experimental spectrum. The full PDF is written as

$$f(m_i)=\frac{N_0}{C(m_i)}[R\cdot H(m_i;M_{J/\psi},\sigma_G)+1+a(m_i-M_{J/\psi})+b(m_i-M_{J/\psi})^2], \tag{6}$$

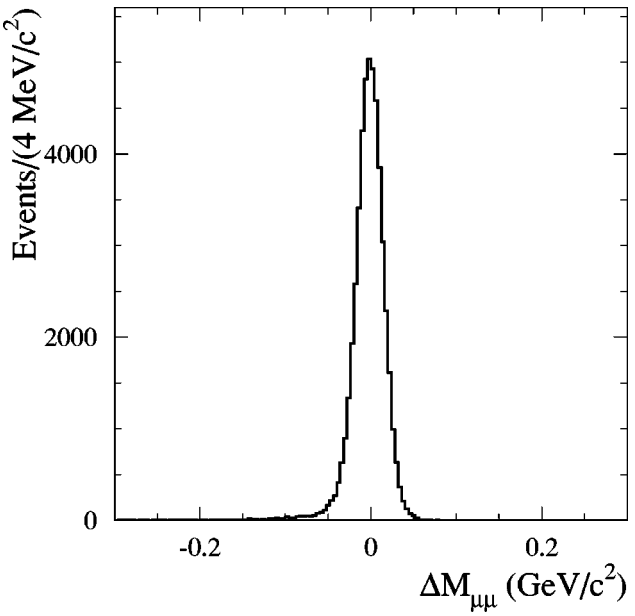

FIG. 4. The distribution of the reconstructed mass minus the generated mass in Monte Carlo events.

where m_i is the central value of the ith bin of the data histogram, $N_0=dN/dm\cdot\Delta m$ is the level of the nonresonant mass distribution at $m=M_{J/\psi}$, $\Delta m=4$ MeV/c^2 is the bin width, H is the PDF for the J/ψ signal with detector resolution, and a and b are the background polynomial coefficients. To account for the interference between resonant and nonresonant amplitudes described in Eq. (5), the PDF is divided by the correction function $C(m_i)$, which is the ratio of the di-muon mass spectra calculated with and without interference as shown in Fig. 2. Because the shape of this function depends on the J/ψ parameters (mass, full width), an iterative procedure is used to calculate it. The ratio

$$R=\frac{N_{J/\psi}}{\frac{dN}{dm}\cdot\Delta m} \tag{7}$$

is the main fit parameter. Here $N_{J/\psi}$ is the number of observed J/ψ decays. After substituting cross sections for numbers of events, this ratio can be rewritten

$$R=\frac{\sigma^{\rm Born}_{J/\psi}}{\frac{d\sigma^{\rm Born}_{\rm ISR}}{dm}\Delta m}\frac{1}{K},\quad K=\frac{d\sigma^{\rm vis}_{\rm Total}/dm}{d\sigma^{\rm vis}_{\rm ISR}/dm}. \tag{8}$$

Detector acceptances and radiative corrections to the initial particles are the same for nonresonant and J/ψ contributions to ISR production of $\mu^+\mu^-\gamma$ and cancel in the ratio. The total nonresonant cross section includes FSR contributions, which we parametrize in terms of K, the ratio of the visible nonresonant total and ISR-only (FSR switched off) cross sections. Using simulated events, we determine $K=1.11\pm0.01$ (statistical error only) for our selection criteria.

TABLE I. The sources of systematic errors in $R \cdot K$.

Statistical error of K factor	0.9%
Systematic error of K factor	1.3%
Background uncertainty	0.5%
Simulation of J/ψ line shape	1.4%
Interference effect	0.3%
Total	2.2%

The result of the fit is shown in Fig. 3. We find $R = 18.94 \pm 0.44$ with χ^2 per degree of freedom $\chi^2/\nu = 122/144$. This fitted value of R must be multiplied by 1.002 to correct for nonresonant and resonant contributions from $e^+e^- \to e^+e^-\gamma$, $\pi^+\pi^-\gamma$, $K^+K^-\gamma$.

The nonresonant cross section extracted from this measurement is close to the value expected from simulation. Their ratio is 0.968 ± 0.016. The quoted uncertainty includes a 0.4% statistical error, a 1% statistical error from simulation, and a 1.2% uncertainty in luminosity. We have not studied the systematic uncertainties on the efficiency for the nonresonant process in detail, as most of these cancel in R and, hence, do not affect the measurement of the J/ψ parameters.

The fitted value of $M_{J/\psi}$ is shifted from that in the simulation by $-(1.6 \pm 0.3)$ MeV/c^2. The fitted value of σ_G is 3.4 ± 1.4 MeV/c^2, corresponding to an overall mass resolution (≈ 14.5 MeV/c^2) 3% larger than that of the simulation. The background slope a corresponds to a 10% change of the nonresonant cross section in the mass range from 2.8 to 3.4 GeV/c^2. The value of b is consistent with zero, in agreement with the Monte Carlo calculation.

As seen in Eq. (8), the ISR J/ψ production cross section is proportional to the product of R, determined from fitting the data, and K, determined from Monte Carlo simulations. The primary sources of systematic uncertainties for the product $R \cdot K$ are summarized in Table I. Uncertainty in K is caused by different detection efficiencies for the pure ISR process of J/ψ production and the nonresonant $e^+e^- \to \mu^+\mu^-\gamma$ process to which both ISR and FSR amplitudes contribute. We estimate the uncertainty due to data–Monte Carlo differences by studying the stability of $R \cdot K$ for different selection criteria. We vary the photon and muon angular selection criteria and the muon momentum requirement over a wide range of values. While the value of K varies from 1.08 to 1.19, the maximum deviation from our reference mean value $R \cdot K = 21.03$ is only 1.3%. Although this variation might be a statistical fluctuation (at least in part), we treat it as a systematic uncertainty associated with the value of K.

As described earlier, we use Monte Carlo simulations of specific ISR and other processes to estimate the level of nonresonant background to be less than 0.4%. We also use the data themselves to estimate this quantity. We compare the fit results for data selected with the standard selection criteria and for data selected with additional muon identification for one of the charged particles. This reduces pion (kaon) contamination by a factor of 9 (3). From the difference in $R \cdot K$, we estimate that the level of nonresonant background does not exceed 0.5%.

The fit results do depend significantly on the model assumed for the J/ψ line shape. The shape of the signal distribution varies with the selection of the maximum allowed value of the χ^2 from the one-constraint fit. Requiring lower values tends to reject events with extra photons, thus reducing the fraction of events in the low mass tail of the J/ψ peak. The fraction of J/ψ events with mass less than $(M_{J/\psi} - 0.1)$ GeV/c^2 changes from 2.4% for no χ^2 cut, to 0.4% for $\chi^2 < 5$. Refitting data with different requirements on the value of χ^2 does not change the result for $R \cdot K$ significantly. The maximum deviation of $R \cdot K$ from our reference mean value, 1.4%, is taken as a systematic uncertainty.

We also consider an additional contribution to the lineshape uncertainty by refitting the data with a model that does not include interference between the nonresonant and J/ψ production amplitudes. The quality of this fit is good: $\chi^2/\nu = 138/144$. As the data do not distinguish between the two models statistically, we take the difference in R, 0.3%, as the corresponding systematic uncertainty. The total systematic error for $K \cdot R$ is 2.2%, compared to the statistical error of 2.3%.

The Born cross section for the process $e^+e^- \to J/\psi\,\gamma \to \mu^+\mu^-\gamma$ can be evaluated from Eq. (8). The nonresonant Born cross section in this formula is calculated to be $d\sigma_{\rm ISR}^{\rm Born}/dm \cdot 4$ MeV/$c^2 = 101.0$ fb. Following the generally accepted practice [14] of including the vacuum polarization correction in the value of the electron width Γ_{ee}, we multiply the pure Born cross section by 1.042 ± 0.002. From $R \cdot K = 21.03 \pm 0.49 \pm 0.47$ we calculate the cross section $\sigma_{J/\psi} = 2124 \pm 49 \pm 47$ fb and the product of the J/ψ parameters

$$\Gamma_{ee} B_{\mu\mu} = 0.3301 \pm 0.0077 \pm 0.0073 \ \text{keV}.$$

From the PDG values [2] for B_{ee} and $B_{\mu\mu}$, which are dominated by those measured in $\psi(2S) \to J/\psi\pi^+\pi^-$ decays by the BES Collaboration [8], we derive the electronic and total widths of the J/ψ meson,

$$\Gamma_{ee} = 5.61 \pm 0.20 \ \text{keV}, \quad \Gamma = 94.7 \pm 4.4 \ \text{keV},$$

using the correlated errors reported by BES. The statistical and systematic uncertainties are combined in quadrature. Our results agree with the previous world averages [2], $\Gamma_{ee} = 5.26 \pm 0.37$ keV and $\Gamma = 87 \pm 5$ keV, but are more precise.

We are grateful for the excellent luminosity and machine conditions provided by our PEP-II colleagues, and for the substantial dedicated effort from the computing organizations that support BABAR. The collaborating institutions wish to thank SLAC for its support and kind hospitality. This work is supported by DOE and NSF (USA), NSERC (Canada), IHEP (China), CEA and CNRS-IN2P3 (France), BMBF and DFG (Germany), INFN (Italy), FOM (The Netherlands), NFR (Norway), MIST (Russia), and PPARC (United Kingdom). Individuals have received support from the A. P. Sloan Foundation, Research Corporation, and Alexander von Humboldt Foundation.

[1] See, for example, A.B. Arbuzov *et al.*, J. High Energy Phys. **12**, 009 (1998); S. Binner, J.H. Kuehn, and K. Melnikov, Phys. Lett. B **459**, 279 (1999); M. Benayoun *et al.*, Mod. Phys. Lett. A **14**, 2605 (1999).
[2] Particle Data Group, K. Hagiwara *et al.*, Phys. Rev. D **66**, 010001 (2002).
[3] BABAR Collaboration, B. Aubert *et al.*, Nucl. Instrum. Methods Phys. Res. A **479**, 1 (2002).
[4] PEP-II Conceptual Design Report, SLAC-R-418, 1993.
[5] See, for example, F.A. Berends and G.J. Komen, Nucl. Phys. **B115**, 114 (1976).
[6] T.A. Armstrong *et al.*, Phys. Rev. D **47**, 772 (1993).
[7] BES Collaboration, J.Z. Bai *et al.*, Phys. Lett. B **355**, 374 (1995).
[8] BES Collaboration, J.Z. Bai *et al.*, Phys. Rev. D **58**, 092006 (1998).
[9] J. Milana, S. Nussinov, and M.G. Olsson, Phys. Rev. Lett. **71**, 2533 (1993).
[10] T. Sjostrand, Comput. Phys. Commun. **82**, 74 (1994).
[11] A.B. Arbuzov *et al.*, J. High Energy Phys. **10**, 001 (1997).
[12] M. Caffo, H. Czyz, and E. Remiddi, Nuovo Cimento Soc. Ital. Fis., A **110A**, 515 (1997); Phys. Lett. B **327**, 369 (1994).
[13] E. Barberio, B. van Eijk, and Z. Was, Comput. Phys. Commun. **66**, 115 (1991).
[14] Crystal Ball Collaboration, Z. Jakubowski *et al.*, Z. Phys. C **40**, 49 (1988).